

The circular polarization of the Mn I resonance lines around 280 nm for exploring chromospheric magnetism

TANAUSÚ DEL PINO ALEMÁN,^{1,2} ERNEST ALSINA BALLESTER,^{1,2} AND JAVIER TRUJILLO BUENO^{1,2,3}

¹*Instituto de Astrofísica de Canarias, E-38205 La Laguna, Tenerife, Spain*

²*Departamento de Astrofísica, Universidad de La Laguna, E-38206 La Laguna, Tenerife, Spain*

³*Consejo Superior de Investigaciones Científicas, Spain*

ABSTRACT

We study the circular polarization of the Mn I resonance lines at 279.56, 279.91, and 280.19 nm (hereafter, UV multiplet) by means of radiative transfer modeling. In 2019, the CLASP2 mission obtained unprecedented spectropolarimetric data in a region of the solar ultraviolet including the Mg II h and k resonance lines and two lines of a subordinate triplet, as well as two Mn I resonance lines. The first analysis of such data, in particular those corresponding to a plage region, allowed the inference of the longitudinal magnetic field from the photosphere to the upper chromosphere just below the transition region. This was achieved by applying the weak field approximation to the circular polarization profiles of the Mg II and Mn I lines. While the applicability of this approximation to the Mg II lines was already demonstrated in previous works, this is not the case for the Mn I UV multiplet. These lines are observed as absorptions between the Mg II h and k lines, a region whose intensity is shaped by their partial frequency redistribution effects. Moreover, the only Mn I stable isotope has nuclear spin $I = 5/2$ and thus hyperfine structure must be, a priori, taken into account. Here we study the generation and transfer of the intensity and circular polarization of the Mn I resonance lines accounting for these physical ingredients. We analyze their sensitivity to the magnetic field by means of their response function, and we demonstrate the applicability of the weak field approximation to determine the longitudinal component of the magnetic field.

Keywords: Solar chromosphere - Radiative transfer - Spectropolarimetry - Magnetic fields

1. INTRODUCTION

The solar chromosphere extends over 10–20 pressure scale heights between the comparatively cold and dense photosphere and the million-degree rarefied corona (see Carlsson et al. 2019, and references therein). It is within the chromosphere where, on average, the magnetic pressure finally overcomes the exponentially decreasing gas pressure and thus the magnetic field starts dominating the dynamics and structuring of its plasma. It is thus clear that understanding the chromospheric magnetic field is essential to fully understanding the physics of this region of the solar atmosphere.

The results of theoretical spectropolarimetric investigations of ultraviolet (UV) chromospheric lines (see Trujillo Bueno et al. 2017, and references therein) led to the CLASP (Chromospheric Lyman Alpha SpectroPolarimeter; Kano et al. 2012) and CLASP2 (Chromospheric LAYER SpectroPolarimeter; Narukage et al. 2016) suborbital rocket experiments. The former successfully measured the intensity and linear polarization in the hydrogen Lyman- α line in a quiet Sun region (Kano et al. 2017), while the latter achieved full Stokes measurements in the UV region around the Mg II h and k resonance lines (between approximately 279.4 and

280.6 nm) in both a plage (Ishikawa et al. 2021) and quiet Sun (Rachmeler et al. 2022) regions.

The CLASP2 plage observations revealed significant fractional circular polarization signals of several percent, not only in the Mg II spectral lines but also in two of the Mn I spectral lines in the observed range, namely, two resonance lines at 279.91 and 280.19 nm. The application of the weak field approximation (WFA) to those profiles allowed the inference of the longitudinal component of the magnetic field at three different regions of the solar chromosphere. The inner (outer) lobes of the Mg II h & k lines are sensitive to magnetic fields in the upper (mid) chromosphere (del Pino Alemán et al. 2020), while the Mn I lines are sensitive to the magnetic field in lower regions of the solar chromosphere. While the height of formation and applicability of the WFA to the Mg II lines have been the subject of several studies (Alsina Ballester et al. 2016; del Pino Alemán et al. 2016; Afonso Delgado et al. submitted), this is not the case for the Mn I lines.

In Ishikawa et al. (2021) we advanced that, indeed, the WFA can be applied to these Mn I lines and that “A non-LTE radiative transfer investigation that will be published elsewhere shows that the V/I signals of

such Mn I lines originate in the lower chromosphere, near the temperature minimum region in standard solar semi-empirical models”. Here we provide such a demonstration. The Mn I resonance lines are observed as absorptions in the spectral region between the Mg II h and k lines. That region of the intensity spectrum is severely affected by partial frequency redistribution (PRD) effects in Mg II (Uitenbroek 1997). It is thus necessary to model both multiplets simultaneously, while accounting for PRD effects in Mg II. Moreover, the only stable isotope of Mn I has nuclear spin $I = 5/2$ and, therefore, hyperfine structure (HFS) must be, a priori, taken into account.

Some Mn I lines have been previously studied in the literature, accounting for the HFS. López Ariste et al. (2002) and Asensio Ramos et al. (2007) studied some of the visible and near-infrared Mn I lines by assuming a Milne-Eddington atmosphere. Bergemann & Gehren (2007) carried out non-LTE intensity calculations, demonstrating the impact of non-LTE effects on the ionization balance, in relatively complex Mn I atomic models. Bergemann et al. (2019) carried out a non-LTE study of the formation of Mn I lines in late-type stars, including the development of an atomic model with new and refined atomic data. However, none of these previous investigations studied the formation of the Mn I chromospheric UV lines.

In this work we model the circular polarization profiles of the Mn I resonance lines at 279.56, 279.91, and 280.19 nm (hereafter, UV multiplet) together with the Mg II h & k lines, accounting for HFS in the former and PRD effects in the latter. In Section 2 we briefly describe the physical problem and the method of solution. In Section 3 we describe the atomic models used in this work and show the height of formation of the Mn I resonant multiplet. In Section 4 we show the results of our radiative transfer (RT) modeling, studying the effect of the HFS and the applicability of the WFA. Finally, we summarize our conclusions in Section 5.

2. PHYSICAL PROBLEM

We solve the problem of the generation and transfer of polarized radiation to model the circular polarization in the Mn I UV multiplet. Mn I is a minority species that shows nonlocal thermodynamic equilibrium effects in its spectral lines radiation. Relatively large model atoms, in terms of the number of atomic levels and transitions, are required to correctly compute the population balance (e.g, Bergemann et al. 2019 for the Mn I atom; Shchukina & Trujillo Bueno 2001 for the similar Fe I atom). We defer the description of the atomic models to §3. There is an additional complication in the mo-

deling of this multiplet, namely, that the spectral lines are located in the spectral region between the Mg II h & k lines and, while not blended with the strong emission peaks around the core of these strong transitions, they are in a region of the spectrum significantly affected by PRD effects in Mg II. Thus, the Mn I UV multiplet appears as absorption lines on the wing pattern of the Mg II h & k lines. Consequently, we need, a priori, to include both atoms in our modeling of the circular polarization, taking into account PRD effects in the Mg II h & k doublet.

Moreover, Mn has only one isotope with nuclear spin $I = 5/2$ and, therefore, HFS must be accounted for. In the presence of a magnetic field, the HFS levels split into their magnetic components. The HFS F-levels are relatively close in energy and magnetic field strengths of 10 G and 80 G are enough to induce repulsion and crossing among the magnetic levels in the lower (a^6S) and upper (y^6P^o) terms, respectively (see Fig. 1). Therefore, it is important to consider the general incomplete Paschen-Back effect regime. Due to the complexity of the problem and the lack of a general RT code capable of taking into account all the above-mentioned physical ingredients, we have opted for the following modeling strategy:

- 1 Compute with the HanleRT code (del Pino Alemán et al. 2016) the population balance using relatively extensive atomic models for the Mn I and Mn II atoms neglecting HFS while including a suitable Mg II atomic model, taking into account PRD effects in its resonance transitions.
- 2 Fix the populations of the two Mn I terms of the multiplet of interest and solve the problem of the generation and transfer of polarized radiation for a Mn I two-term atom together with the Mg II ion applying the HanleRT code. We solve the problem with and without accounting for HFS, but always neglecting quantum interference between the hyperfine F -levels.
- 3 Taking the resulting radiation field tensors, emissivity and absorptivity contributions of the Mg II h & k lines, and the population of the a^6S Mn I term, solve the two-term problem with HFS and J - and F - state quantum interference with the code developed by Alsina Ballester et al. (2022), thus accounting for all relevant physical ingredients, including the Paschen-Back effect. Note that for this step we do not solve the self-consistent RT problem but instead use the results from the second step to

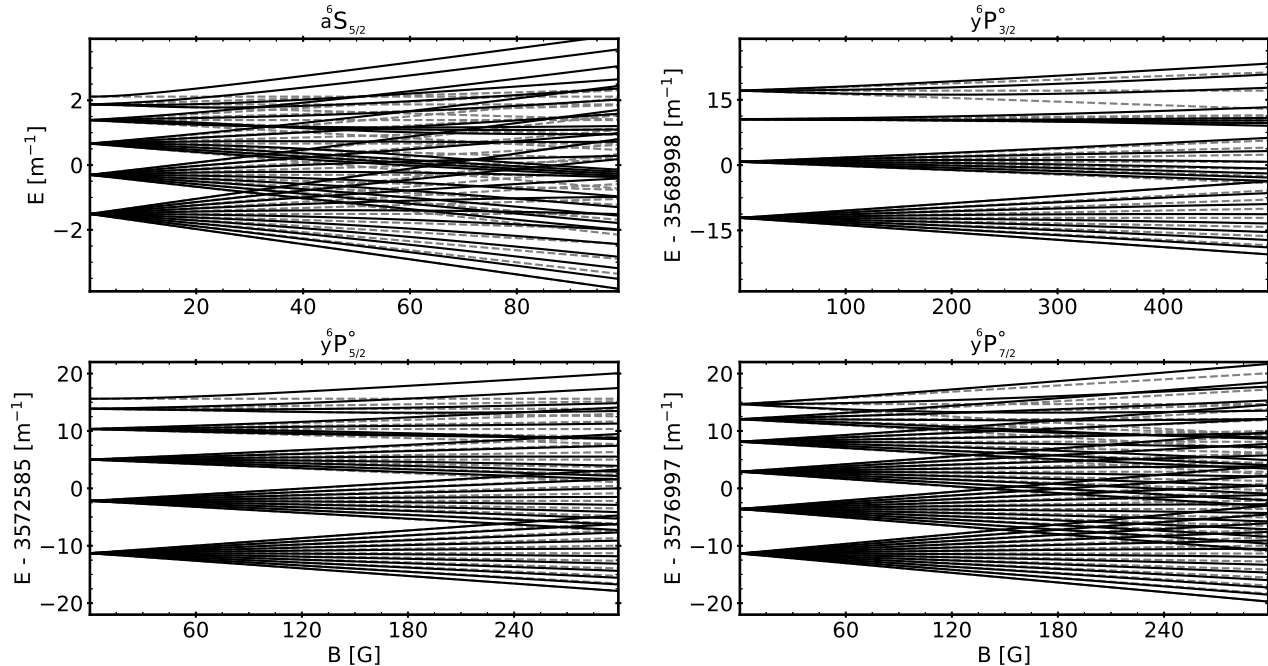


Figure 1. The energy of the HFS levels corresponding to each of the atomic levels, indicated above each panel, of the Mn I resonance lines, for different magnetic fields (black solid curves). The gray dashed lines show the same, but with the linear Zeeman approximation.

obtain a single formal solution along the lines of sight (LOS) of interest.

3. ATOMIC MODEL AND HEIGHT OF FORMATION

We compute the population balance using an atomic model with 319 Mn I levels and 318 transitions, 525 Mn II levels and 891 transitions, and the ground term of Mn III (see Fig. 2). These correspond to all levels and transitions available in the NIST database (Kramida et al. 2018), from where we took the atomic level energies and oscillator strengths. We accounted for quadratic Stark and collisional broadening in the spectral lines with the C_6 and C_4 estimates without enhancements (Mihalas 1978). We included hydrogenic photoionization cross sections (e.g., Mihalas 1978). The excitation rate due to inelastic collisions with electrons between levels radiatively connected by an electric dipole transition was computed following van Regemorter (1962), while Bely & van Regemorter (1970) was followed for the rest of the level pairs, taking the parameter $\Omega = 0.1$. Ionizing rates due to inelastic collisions with electrons were computed following Allen (1963). Although these are relatively rough approximations, they are suitable for the purposes of this paper.

The two-term atomic model we use to compute the polarization of the Mn I resonance lines includes the three levels of the upper y^6P term, with total angular momen-

tum $J = 3/2, 5/2,$ and $7/2,$ and the single level of the lower $a^6S_{5/2}$ term. There are three transitions connecting each of the levels of the upper term with the lower level (see the left panel in Fig. 3). We solve the RT problem for this multiplet in the semiempirical P model of Fontenla et al. (1993, hereafter FAL-P) following steps 1 and 2 of the procedure described in §2. We have chosen the FAL-P model because it is representative of a plage region, such as that observed by the CLASP2 mission. In Fig. 4 we show the intensity contribution function (e.g., Uitenbroek 2006) for the Mn I UV multiplet lines, as well as the circular polarization response function (Magain 1986), for the same lines and for a spectral range that also includes the Mg II h-k and subordinate triplet lines. The response function indicates how the circular polarization profile responds to changes in the magnetic field at each layer in the model atmosphere, and thus shows where in the model atmosphere is the emergent circular polarization profile sensitive to the magnetic field. The Mn I lines at 279.91 and 280.19 nm are thus sensitive to magnetic fields at heights between about 500 and 900 km in the FAL-P model, which corresponds to the lower chromosphere in that model. The response of the Mn I line at 279.56 nm is more concentrated toward the higher part of this range but, unfortunately, this line is blended with the blue wing of the Mg II k line. The faint blue response in the outer wings of the Mn I line at 279.56 nm corresponds to the Mg II

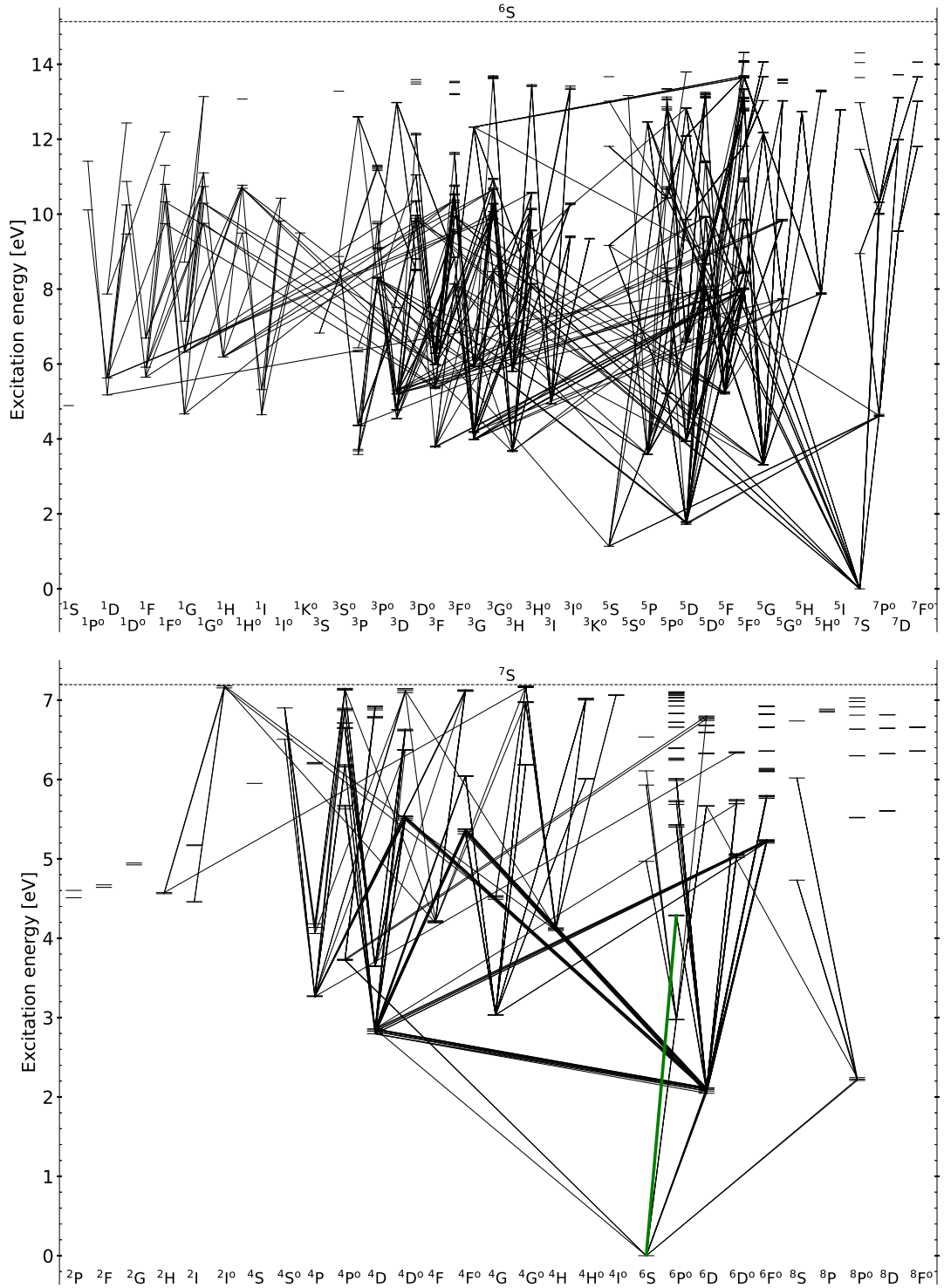


Figure 2. Grotrian diagram of the atomic models for the Mn I (bottom panel) and the Mn II (top panel) atoms used to calculate the population balance. The solid lines show the considered radiative transitions. Every atomic level is connected to every other level via inelastic collisions with electrons and every Mn I level is connected with the ground term of Mn II via photoionization and recombination (these transitions are not shown in the diagrams for a better visualization). The green line shows the transition corresponding to the Mn I UV multiplet. The horizontal dashed lines show the ionization energy for each corresponding atomic species, with the atomic configuration of the ground term of the next ionization stage.

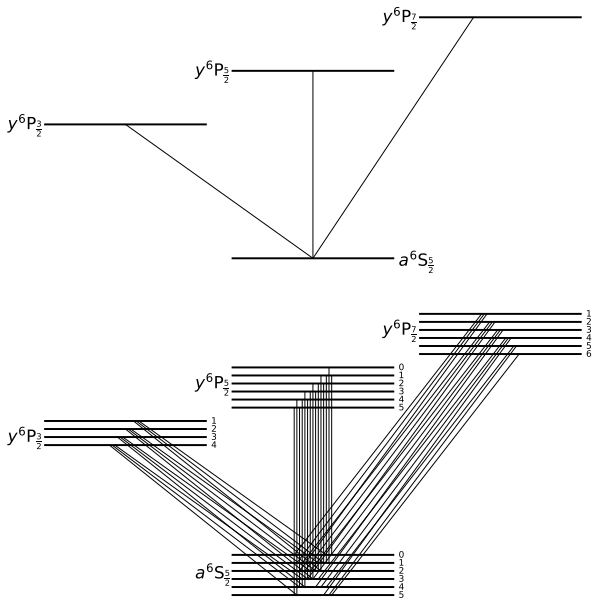


Figure 3. Grotrian diagram for the Mn I UV multiplet neglecting (top panel) and accounting for (bottom panel) HFS. The four J-levels radiatively coupled by three transitions become 22 F-levels connected by 42 transitions.

k line. Note that the response function for each panel is normalized to the maximum in the wavelength range of the corresponding panel. In the full wavelength range (including both the Mg II resonant doublet and the Mn I UV multiplet) the maximum of the response function is in the Mg II h and k lines and thus the response function in the bottom panel is normalized to a value larger than those in the individual panels for each of the Mn I lines. This is the reason why the relatively small positive response in the k line wing around the Mn I line at 279.56 nm is seen in the left panel in the middle row, but not in the bottom panel. In the calculation of these contribution and response functions we have neglected HFS, but we do not expect a significant impact on the height of formation by including its contribution.

When accounting for the HFS, each J level splits into $(I+J) - |I-J| + 1$ hyperfine levels. The HFS model thus has 22 levels, with 42 electric dipole transitions (see the right panel in Fig. 3). The energy for each F level in the model atom with HFS is given by Arimondo et al. (1977)

$$E_{LJF} = E_{LJ} + A \frac{K}{2} + B \frac{\frac{3}{2}K(K+1) - 2I(I+1)J(J+1)}{2I(2I-1)2J(2J-1)}, \quad (1)$$

where

$$K = F(F+1) - J(J+1) - I(I+1), \quad (2)$$

and A and B are the HFS constants given in Table 1.

Table 1. Hyperfine structure constants for the atomic levels of the Mn I UV multiplet.

Term	J	E_{LJ} (cm $^{-1}$)	A (cm $^{-1}$)	B (cm $^{-1}$)
$a^6S^{(1)}$	5/2	0	-2.416e-3	-6.348e-7
$y^6P^{(2)}$	3/2	35689.98	-3.24e-2	1.1e-3
	5/2	35725.85	-1.80e-2	-2.0e-3
	7/2	35769.97	-1.30e-2	9.0e-4

(1) Davis et al. (1971)

(2) Luc & Gerstenkorn (1972)

4. RESULTS

In this section we show the results of our RT calculations, analyzing the impact of the HFS on the Mn I UV multiplet Stokes profiles, as well as the applicability of the WFA to the circular polarization profiles to infer the longitudinal component of the magnetic field.

4.1. Hyperfine structure

We have solved the RT problem for the Mg II h and k lines, its subordinate triplet at 279.88 nm, and the Mn I UV multiplet following the procedure outlined in §2, both with and without accounting for HFS, in the FAL-P model permeated by a constant 500 G vertical magnetic field (see Fig. 5). Concerning the intensity profile, the inclusion of the HFS increases its broadening due to the spread in the energy of the F-levels. Regarding the circular polarization profile (red curves), not only are the lobes shifted away from the line center (as expected due to the broader intensity profile), but their value is decreased with respect to the no-HFS case, as would also be expected if the circular polarization profile were proportional to the derivative of the intensity. It is important to emphasize the necessity of accounting for the Paschen-Back effect to correctly model the circular polarization profile; if the energies of the magnetic sub-levels of the atomic system are assumed to vary linearly with the magnetic field strength (red dotted curve), the circular polarization in the Mn I lines at 279.91 and 280.19 nm is significantly underestimated.

4.2. Weak field approximation

The main motivation for this investigation is testing the validity of the WFA to infer the longitudinal component of the magnetic field. To this end, we compare the circular polarization profile obtained from our RT calculation with the profile obtained with the WFA, namely (e.g., Landi Degl'Innocenti & Landolfi 2004),

$$V(\lambda) = -4.6686 \cdot 10^{-13} \lambda_0^2 \bar{g} B_{\text{LOS}} \frac{\partial I}{\partial \lambda}, \quad (3)$$

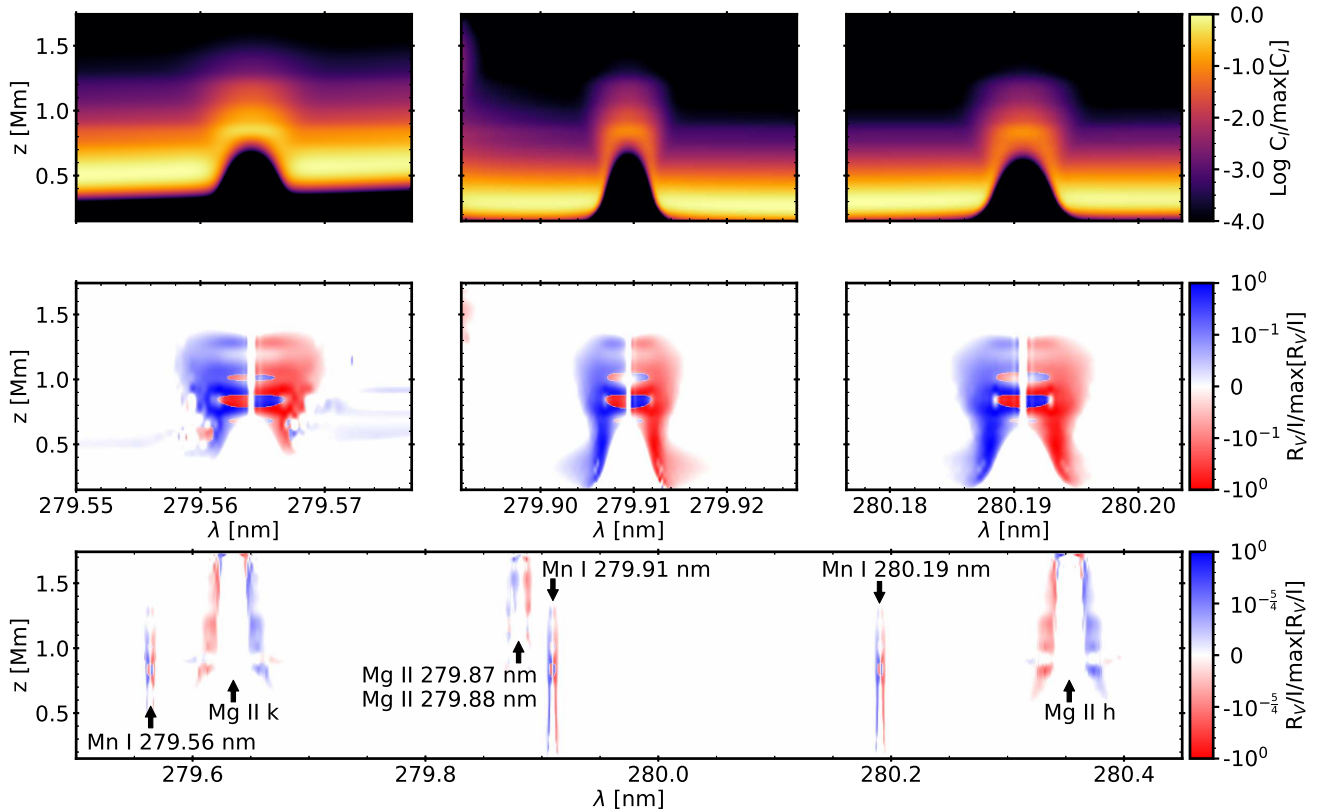


Figure 4. Intensity contribution function (top row) and circular polarization response function (middle row) for the three lines of the Mn I UV multiplet (ordered from left to right for increasing wavelength) in the FAL-P semiempirical model with a constant vertical 100 G magnetic field, neglecting HFS. The panel in the bottom row shows the circular polarization response function for the wavelength range including the Mn I UV multiplet and the Mg II h and k lines and subordinate lines at 279.88 nm. We show the logarithm of the contribution and response functions normalized to the maximum for each wavelength range. For the circular polarization, the red (blue) color indicates that the response to the circular polarization is negative (positive).

where λ_0 is the transition wavelength in \AA , B_{LOS} is the longitudinal component of the magnetic field in gauss, and \bar{g} is the effective Landé factor of the transition. The \bar{g} values of the lines of the Mn I UV multiplet, in wavelength order, are 1.36, 1.94, and 1.70. Assuming that the contribution to the Doppler width is purely thermal and assuming a lower boundary of the temperature of 4000 K, the ratio between Zeeman splitting and Doppler width is, for the Mn I line at 279.56 nm (the one with the smallest effective Landé factor), equal or smaller than unity for magnetic fields with $|B| \lesssim 2$ kG (e.g., this ratio is ≈ 0.3 for $|B| = 500$ G). Therefore, in terms of magnetic field strengths, the WFA approximation is expected to be applicable to these lines for the typical physical properties of the solar plasma.

When neglecting HFS, the WFA profiles fit the emergent circular polarization (see top row of Fig. 6). Likewise, when accounting for the HFS (see black curves in the bottom row of Fig. 6), the WFA also fits the circular polarization profile, thus validating its use to infer the

longitudinal component of the magnetic field for weak magnetic fields. However, as advanced in §4.1, it is important to note that this fit can only be demonstrated if the RT problem is solved accounting for all the relevant physical ingredients, namely HFS in the incomplete Paschen-Back regime. To illustrate the latter, we have also included the Mn I multiplet circular polarization profiles calculated in the linear Zeeman regime (see red curves in the bottom row of Fig. 6). In the third step of the modeling (see Sect. 2) this regime was attained by neglecting the off-diagonal elements of the magnetic Hamiltonian, so that the energies of the magnetic sub-levels vary linearly with the magnetic field strength. Under such an approximation the circular polarization profile is underestimated and one could reach the wrong conclusion that the WFA profile does not fit the circular polarization. It is also important to emphasize that the WFA profiles in the bottom row of Fig. 6 (with HFS) have been calculated using the effective Landé factors of the transition neglecting the HFS. This is an example

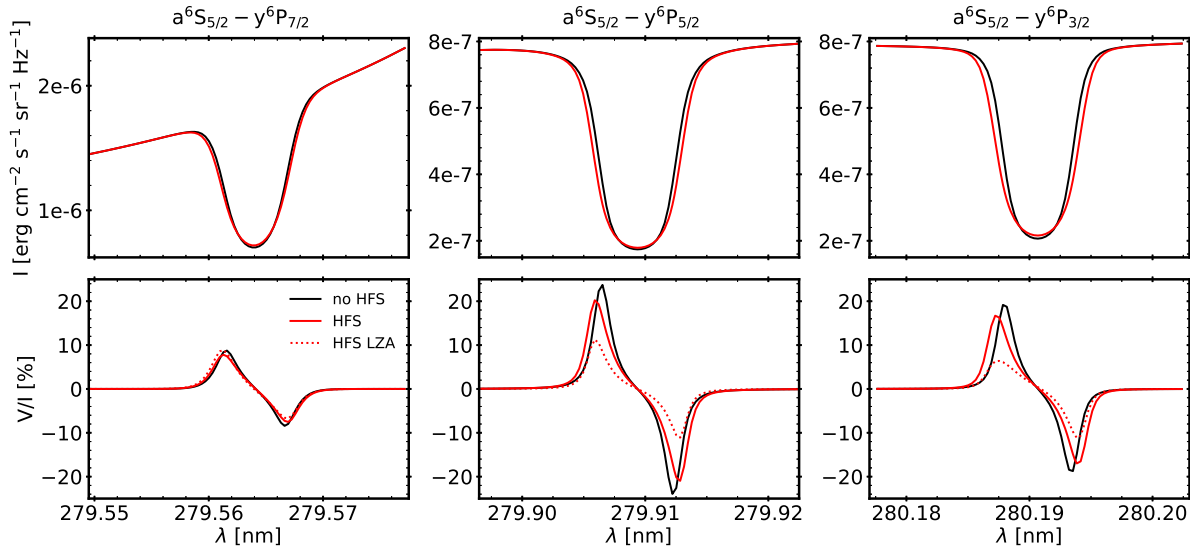


Figure 5. Intensity (top panels) and fractional circular polarization V/I (bottom panels) profiles for a LOS at the solar disk center, computed in the FAL-P model with a vertical magnetic field of 500 G following the procedure described in §2. The different columns show the lines of the Mn I UV multiplet ordered by their wavelength from left to right. The black (red) solid curve shows the calculation neglecting (accounting for) HFS. The red dotted curve shows the circular polarization profile in the linear Zeeman approximation (i.e., assuming that the energies of the various magnetic sublevels depend linearly on the magnetic field strength), which significantly underestimates the circular polarization amplitude in two of the Mn I resonance lines.

of the principle of spectroscopic stability: “if two different descriptions are used to characterize a quantum system – a detailed description which takes an inner quantum number into account and a simplified description which disregards it – the predicted results must be the same in all physical experiments where the structure described by the inner quantum number is unimportant” (Landi Degl’Innocenti & Landolfi 2004). The differences in energy between the HFS F-levels of each J-levels are thus small enough to satisfy this principle.

5. CONCLUSIONS

We have studied the formation of the circular polarization profiles of the Mn I UV multiplet taking into account its HFS as well as PRD effects in the Mg II h and k lines that shape the intensity “continuum” on top of where the Mn I absorptions are observed. From the response function to perturbations to the longitudinal component of the magnetic field we have shown that the circular polarization of the Mn I resonant triplet is sensitive to the magnetic field in a more or less extensive region around 900 km in the FAL-P model atmosphere, which corresponds to its lower chromosphere. This justifies the decision to assign the magnetic field inferred from the application of the WFA to the Mn I circular polarization profiles to the lower chromosphere in Ishikawa et al. (2021).

While the HFS energy splitting slightly broadens the Mn I triplet intensity profiles, its impact on the circular

polarization profiles is more evident, shifting its lobes further from the line core and slightly reducing their amplitude. We have demonstrated that the linear Zeeman approximation is not suitable to model the Mn I circular polarization profiles with HFS, as it severely underestimates the polarization amplitude.

Finally, the circular polarization profiles obtained by applying the WFA with the known homogeneous magnetic field and the effective Landé factors corresponding to the fine structure transitions (i.e., as if neglecting HFS) fit the circular polarization profiles resulting from the calculations accounting for the incomplete Paschen-Back effect. This demonstrates that the WFA can be used to infer the longitudinal magnetic field component without accounting for HFS because these lines fulfill the principle of spectroscopic stability; i.e., because the HFS energy split is sufficiently small.

We want to emphasize that because we are imposing a homogeneous magnetic field in a static model atmosphere, physical conditions under which the WFA should work, what we have demonstrated is that the WFA is applicable to these lines despite the HFS and their potential interaction with the Mg II h and k wings. Of course, if the magnetic field gradient is too steep across the region of formation, we would run into the usual limitations of the WFA as an inference tool, namely, we would infer a particular value for the longitudinal magnetic field, but we would be unable to pinpoint where along the LOS is such a field localized. However, we can

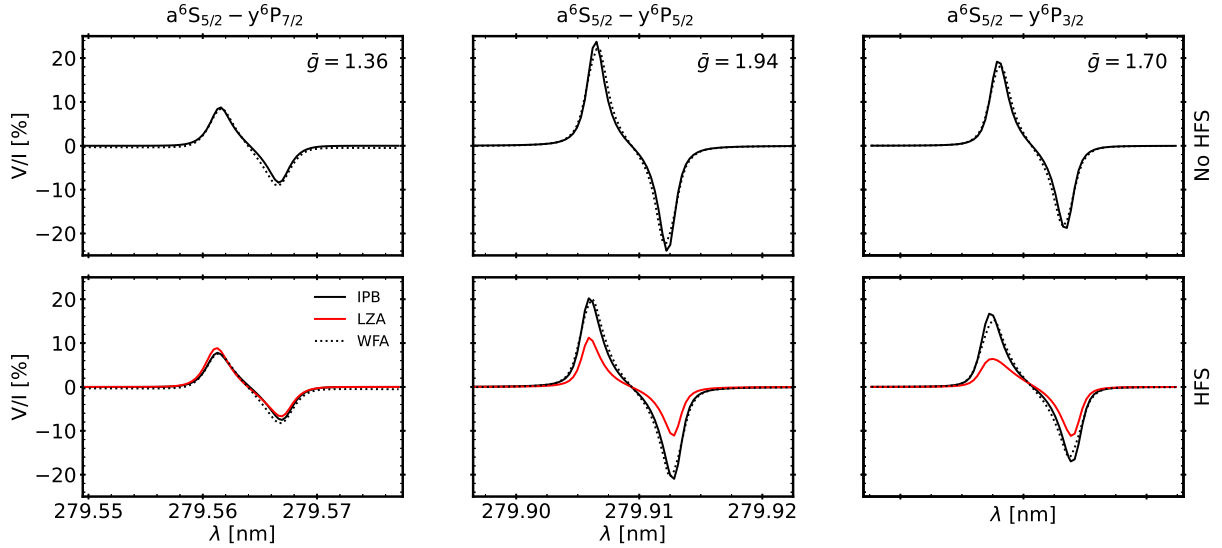


Figure 6. Fractional circular polarization V/I profiles for a LOS at the solar disk center, computed in the FAL-P model with a vertical magnetic field of 500 G following the procedure described in §2. The different columns show the lines of the Mn I UV multiplet ordered by their wavelength from left to right. The black solid curves show the calculation accounting for the incomplete Paschen-Back effect for fine structure (top panels) and for both fine structure and HFS (bottom panels). The red curves in the bottom panels show the result of the calculation assuming the linear Zeeman approximation (LZA; i.e., assuming that the energies of the various magnetic sublevels depend linearly on the magnetic field strength). The black dotted lines show the WFA profile for the same longitudinal magnetic field and the effective Landé factor calculated by assuming LS coupling and neglecting HFS (\bar{g} , indicated in the top panels for each line).

expect that such a magnetic field is at least representative of the magnetic field somewhere across the region of formation of the line, as in Ishikawa et al. (2021).

ACKNOWLEDGMENTS

We acknowledge the funding received from the European Research Council (ERC) under the European Union’s Horizon 2020 research and innovation program (ERC Advanced grant agreement No. 742265).

REFERENCES

- Afonso Delgado, D., del Pino Alemán, T., & Trujillo Bueno, J. submitted
- Allen, C. W. 1963, *Astrophysical quantities*
- Alsina Ballester, E., Belluzzi, L., & Trujillo Bueno, J. 2016, *ApJ*, 831, L15
- . 2022, arXiv e-prints, arXiv:2204.12523
- Arimondo, E., Inguscio, M., & Violino, P. 1977, *Reviews of Modern Physics*, 49, 31
- Asensio Ramos, A., Martínez González, M. J., López Ariste, A., Trujillo Bueno, J., & Collados, M. 2007, *ApJ*, 659, 829
- Bely, O., & van Regemorter, H. 1970, *ARA&A*, 8, 329
- Bergemann, M., & Gehren, T. 2007, *A&A*, 473, 291
- Bergemann, M., Gallagher, A. J., Eitner, P., et al. 2019, *A&A*, 631, A80
- Carlsson, M., De Pontieu, B., & Hansteen, V. H. 2019, *ARA&A*, 57, 189
- Davis, S. J., Wright, J. J., & Balling, L. C. 1971, *PhRvA*, 3, 1220
- del Pino Alemán, T., Casini, R., & Manso Sainz, R. 2016, *ApJL*, 830, L24
- del Pino Alemán, T., Trujillo Bueno, J., Casini, R., & Manso Sainz, R. 2020, *ApJ*, 891, 91
- Fontenla, J. M., Avrett, E. H., & Loeser, R. 1993, *ApJ*, 406, 319

- Ishikawa, R., Bueno, J. T., del Pino Alemán, T., et al. 2021, *Science Advances*, 7, eabe8406
- Kano, R., Bando, T., Narukage, N., et al. 2012, in *Society of Photo-Optical Instrumentation Engineers (SPIE) Conference Series*, Vol. 8443, Proc. SPIE, 84434F
- Kano, R., Trujillo Bueno, J., Winebarger, A., et al. 2017, *ApJ*, 839, L10
- Kramida, A., Yu. Ralchenko, Reader, J., & and NIST ASD Team. 2018, *NIST Atomic Spectra Database* (ver. 5.5.6), [Online]. Available: <http://physics.nist.gov/asd> [May 2018]. National Institute of Standards and Technology, Gaithersburg, MD.
- Landi Degl'Innocenti, E., & Landolfi, M. 2004, *Polarization in Spectral Lines*, Vol. 307 (Kluwer Academic Publishers)
- López Ariste, A., Tomczyk, S., & Casini, R. 2002, *ApJ*, 580, 519
- Luc, P., & Gerstenkorn, S. 1972, *A&A*, 18, 209
- Magain, P. 1986, *A&A*, 163, 135
- Mihalas, D. 1978, *Stellar atmospheres /2nd edition/*
- Narukage, N., McKenzie, D. E., Ishikawa, R., et al. 2016, in *Society of Photo-Optical Instrumentation Engineers (SPIE) Conference Series*, Vol. 9905, Proc. SPIE, 990508
- Rachmeler, L. A., Trujillo Bueno, J., McKenzie, D. E., et al. 2022, *arXiv e-prints*, arXiv:2207.01788
- Shchukina, N., & Trujillo Bueno, J. 2001, *ApJ*, 550, 970
- Trujillo Bueno, J., Landi Degl'Innocenti, E., & Belluzzi, L. 2017, *SSRv*, 210, 183
- Uitenbroek, H. 1997, *SoPh*, 172, 109
- Uitenbroek, H. 2006, in *Astronomical Society of the Pacific Conference Series*, Vol. 354, *Solar MHD Theory and Observations: A High Spatial Resolution Perspective*, ed. J. Leibacher, R. F. Stein, & H. Uitenbroek, 313
- van Regemorter, H. 1962, *ApJ*, 136, 906